Journal of Electrochemistry

Volume 25
Issue 3 *Special Issue: Electrochemical Analysis and Sensing (II)*

2019-06-25

Cysteine and Cystamine Co-Self-Assembled Monolayers for *in Vivo* Detection of Ascorbic Acid

Yue ZHANG

Tao-tao FENG

Wen-liang JI

Mei-ning ZHANG
Department of Chemistry, Renmin University of China, Beijing 100872, China;, mnzhang@ruc.edu.cn

DOI: 10.13208/j.electrochem.181045
Cite this: *J. Electrochem.* **2019**, *25*(3): 400-408

Artical ID:1006-3471(2019)03-0400-09
Http://electrochem.xmu.edu.cn

Cysteine and Cystamine Co-Self-Assembled Monolayers for *in Vivo* Detection of Ascorbic Acid

ZHANG Yue, FENG Tao-tao, JI Wen-liang, ZHANG Mei-ning*
(*Department of Chemistry, Renmin University of China, Beijing* 100872, *China*)

Abstract: Self-assembled monolayers (SAMs), which form highly ordered monolayers on the electrode surface through the gold-suffer bond, have attracted much attention in recent years. This stable layer not only can regulate the wettable properties of surface, but also can act as a promoter towards redox-active molecules. Here, we developed a simple and effective method to construct cysteine and cystamine co-self-assembled monolayer on gold microelectrode for *in vivo* detection of ascorbic acid (AA). The molar ratio at 1:1 of mixed monolayer has been found the optimum to enhance the electron-transfer kinetics of AA oxidation at low potential (ca. 0.10 V), meanwhile, it could resist the non-specific adsorption of protein at electrode surface. The application of the co-self-assembled monolayer is preliminarily demonstrated for *in vivo* detection and the basal level of striatum AA was determined to be 257 ± 30 μmol·L^{-1} (n = 3). This study offers a general and effective approach for *in vivo* electrochemistry with high reliability and simplified procedures.

Key words: cysteine and cystamine; co-self-assembled monolayer; ascorbic acid; anti-adsorption; *in vivo*
CLC Number: O646 **Document Code:** A

Self-assembled monolayers (SAMs) with unique chemical and physical properties have attracted much attention in various fields, such as wettability, biocompatibility, adhesion and sensing[1-6]. As a well-established technology for preparing ultra-thin ordered films, self-assembled membranes not only provide an ideal method to study the surface and interface phenomena, but also provide an effective method to design and obtain specific functional membrane materials[7-8]. Self-assembled membranes of sulfur-containing compounds, especially depending on adsorption by chemical bonds of disulfides (R-S-S-R), sulfides (R-S-R) or thiols (R-SH) on a metal (particularly gold substrates), are the most representative and studied systems[9-10]. Compared with other non-covalently driven self-assembly modes, self-assembly of sulfur compounds on gold surface is formed by polar covalent bonds, and Au-S bonds are easily formed spontaneously, which makes the SAMs have good stability, orderliness and specific electrical, optical or chemical property[11-13].

Due to the high spatial and temporal resolutions, increasing researches have demonstrated that *in vivo* electrochemistry is the important method to analyze small molecular neurochemicals in the central nervous system (CNS)[14-19]. As one of the most important neuromodulators in CNS, AA plays a significant role in maintaining normal physiological function of human body and has wide relationship with the complex components network and brain function *in vivo*[20-22]. However, the high-potential oxidation of AA renders difficulties in selective measurement in CNS because the great interference of other kinds of electroactive species such as 3,4-dihydroxyphenylacetic acid (DOPAC) and uric acid (UA) coexists in the brain. In addition, the brain environment is especially complex, when electrodes are implanted into tissues, proteins will be adsorbed to the surface of electrodes in a non-specific manner, resulting in a decrease in the sensitivity of electrodes[23-24]. Thus, it is very important to establish a rapid and convenient method for *in vivo* detection of AA and resist the protein adsorption in

Received: 2018-12-12, Revised: 2019-03-19 *Corresponding author, Tel: (86-10)62512822, E-mail: mnzhang@ruc.edu.cn

the process of implantation.

Here, we developed a strategy of cysteine and cystamine co-self-assembled monolayer for *in vivo* detection of AA as illustrated in Scheme 1. Cysteine is a kind of zwitterion molecules and a potential anti-protein adsorption material[25-26]. In addition, cysteine was found to be a thin layer (ca. 1.14 nm)[27] that closes to the double layer on the surface of the electrode. Considering the poor selectivity of cysteine for AA, we added cystamine as a promoter to efficiently modulate the electron transfer kinetics of AA oxidation to make the oxidative potential of AA more positive. We found that the co-self-assembled monolayer of cysteine and cystamine at a molar ratio of 1:1 on gold microelectrodes (AuMEs) exhibits good selectivity for *in vivo* detection of AA. Our research provided a potential strategy for *in vivo* electrochemical detection of AA and other neurotransmitter neuromodulator in CNS.

1 Experimental

1.1 Reagents and Solutions

L-cysteine (Cys), cystamine (CYST), and bovine serum albumin (BSA) were purchased from Chemical Reagent Co. Ltd. (Beijing, China). Ascorbic acid (AA), dopamine (DA), 3,4-dihydroxyphenylacetic acid (DOPAC), 5-hydroxytryptamine (5-HT), glutamic acid (Glu), hexaammineruthenium chloride, ferrocene methanol and potassium ferricyanide were purchased from Sigma-Aldrich. The 0.1 mol·L^{-1} phosphate buffer solution containing 50 mmol·L^{-1} NaH_2PO_4 and 50 mmol·L^{-1} Na_2HPO_4 was adjusted to pH 7.4 with sodium hydroxide. Artificial cerebrospinal fluid (aCSF) was prepared by mixing NaCl (126 mmol·L^{-1}), KCl (2.4 mmol·L^{-1}), KH_2PO_4 (0.5 mmol·L^{-1}), $MgCl_2$ (0.85 mmol·L^{-1}), $NaHCO_3$ (27.5 mmol·L^{-1}), Na_2SO_4 (0.5 mmol·L^{-1}), and $CaCl_2$ (1.1 mmol·L^{-1}) into doubly distilled water, and then adjusting the pH to 7.4 as our previous work[23]. All the aqueous solutions were prepared with Milli-Q water. Unless stated otherwise, all experiments were carried out at room temperature.

1.2 Modification of Au Electrodes

Polycrystalline Au electrodes (diameter, 1.5 mm) were immersed in aqua regia to remove the residual contamination, then polished with aqueous slurries of alumina (0.5 and 0.05 μm) and sonicated for 5 ~ 10 min in water. The polished electrodes were then electrochemically pretreated by cycling the potential scan between -0.2 and 1.2 V at 10 V·s^{-1} vs. platinum electrode in 0.5 mol·L^{-1} H_2SO_4 for 10 min until the characteristic cyclic voltamagrams (CVs) for

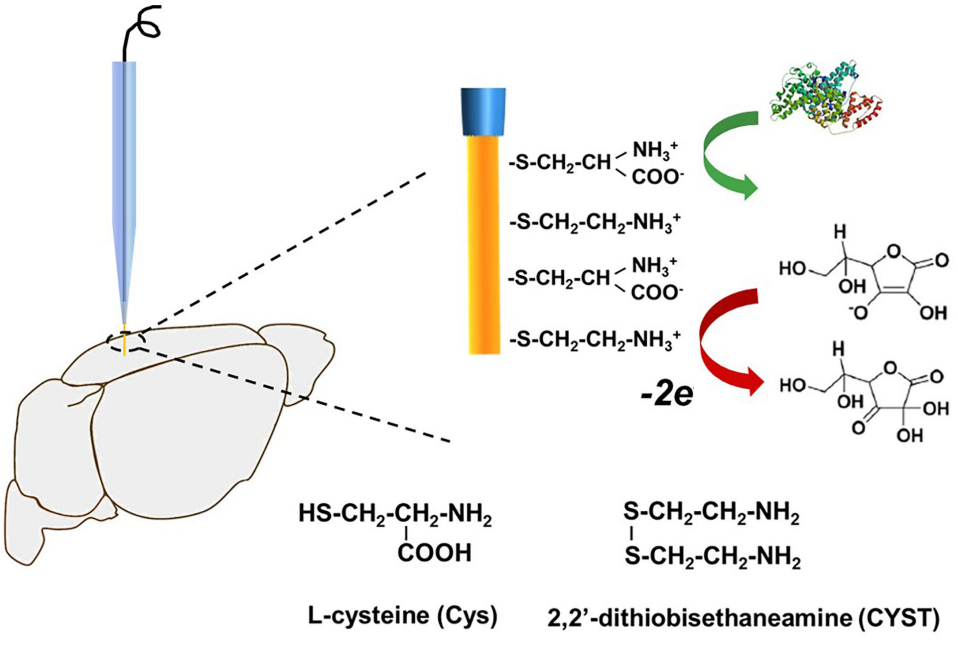

Scheme 1 Schematic of the Cys-CYST/AuMEs for *in vivo* detection of AA

a clean Au electrode was obtained. The Cys/Au and CYST/Au were fabricated by immersing the pretreated Au electrodes into 10 mmol·L^{-1} cysteine and cystamine solutions for 1 h, respectively. The mixed monolayers of cysteine and cystamine were made by soaking the pretreated Au electrodes in solutions containing cysteine and cystamine with different concentrations. The Cys-CYST/Au was formed by immersing the gold electrode in solution containing 10 mmol·L^{-1} cysteine and 10 mmol·L^{-1} cystamine. The electrodes were extracted and washed with a small amount of ultra-pure water, and dried with nitrogen gas before any electrochemical and other tests.

1.3 Fabrication and Modification of Gold Microelectrodes

Gold microelectrodes (AuMEs) were fabricated as reported previously[24]. Briefly, a glass capillary (id. 1.5 mm, length 100 mm) was pulled on a microelectrode puller (WD-2, Chengdu Instrument Factory, Sichuan, China) into two capillaries; the fine tip of each was broken into 30 ~ 50 μm in diameter. The pulled capillary was used as the sheath of AuMEs. A single Au fiber (13 μm in diameter) was attached to copper wire with silver conducting paste. Then, the Au fiber with the attached copper wire was carefully inserted into the capillary with Au fiber being exposed to the fine open end of the capillary and Cu wire being exposed to the other end of the capillary. Both open ends of the capillary were sealed with epoxy resin with 1∶1 ethylenediamine as the harder and the excess epoxy on the fiber was carefully removed with acetone. The exposed Au fiber was cut to 300 ~ 500 μm in length under a microscopy. Prior to modification with monolayer, the fabricated AuMEs were electrochemically pretreated by cycling the potential scan between -0.2 and 1.2 V at 10 V·s^{-1} vs. platinum electrode in 0.5 mol·L^{-1} H_2SO_4 for 10 min until the characteristic CVs for a clean Au electrode was obtained. The method of modification the AuMEs was the same as the gold electrode described above.

1.4 Apparatus and Measurements

The electrochemical measurement was carried out with three-electrode system at room temperature using the computer-controlled CHI 760D electrochemical analyzer (Shanghai Chenhua Instrument Corporation, China). Gold electrode or AuMEs were used as the working electrode, platinum wire as the counter electrode and Ag/AgCl electrode as the reference electrode. The contact angle was measured by JC2000D Contact Angle Measuring Instrument (Shanghai ZhongChen).

1.5 *In Vivo* Experiments

Adult male Sprague-Dawley rats (300 ~ 350 g) were purchased from Health Science Center, Peking University. All animal procedures were approved by the Animal Care and Use Committee at National Center for Nanoscience and Technology of China and performed according to their guidelines. The animals were housed on a 12:12 h light dark schedule with food and water ad libitum. Animal experiments were performed with a method described in our earlier work[28]. Briefly, the animals were anaesthetized with chloral hydrate (345 mg·kg^{-1}, i.p.) and positioned onto a stereotaxic frame. AuMEs were implanted into striatum (AP = 1.5 mm, L = 1.5 mm from bregma, V = 4 mm from dura) using standard stereotaxic procedures[29]. Post-calibration was performed in pure aCSF with successive addition of AA after the microelectrodes were removed from the brain tissue. The concentration of AA was quantitated with post-calibration.

2 Results and Discussion

We first investigated the electrochemical performances of cysteine and cystamine toward AA through the cyclic voltamagrams (CVs), the results are shown in Figure 1A. Typically, at the bare gold electrode, the oxidation peak of AA was ca. 0.35 V vs. Ag/AgCl. The gold electrode with cysteine self-assembled monolayer (Cys/Au) also showed poor response for AA in which oxidation peak was about 0.30 V. In contrast, a large negative shift (ca. 0.3 V) in the peak potential was observed for the oxidation of AA at gold electrode with cystamine self-assembled monolayer (CYST/Au), which was due to the electrostatic interaction as reported previously[30]. We further explored the performance of anti-adsorption

of nonspecific proteins of electrodes above. As shown in Figure 1B, with the BSA being added to AA solution gradually, it was found that the peak current of AA on bare gold electrode decreased significantly, and the peak potential also positively shifted. We found that the CYST/Au had poor anti-protein adsorption performance and the current decreased gradually (Figure 1C). However, the peak current of AA on Cys/Au remained unchanged with the BSA addition, which indicated the good anti-protein adsorption ability of cysteine in protein solution (Figure 1D).

We further explored the optimum ratio of cysteine and cystamine. A series of co-self-assembled monolayers were obtained with different molar ratios (the concentration ratios of cysteine to cystamine were 0.5, 0.75, 1, 2, 3). From the CVs in Figure 2A, the gold electrode with co-assembled monolayer showed good response for AA and the oxidation peak was all at about 0.10 V. We further compared the ability of anti-protein adsorption of gold electrode modified with different ratios of cysteine and cystamine. We added 10 mg·mL^{-1} BSA into 200 μmol·L^{-1} AA solution and compared the oxidation current of AA. It was found that when the molar ratio was 1:1 the anti-protein adsorption performance of the electrode

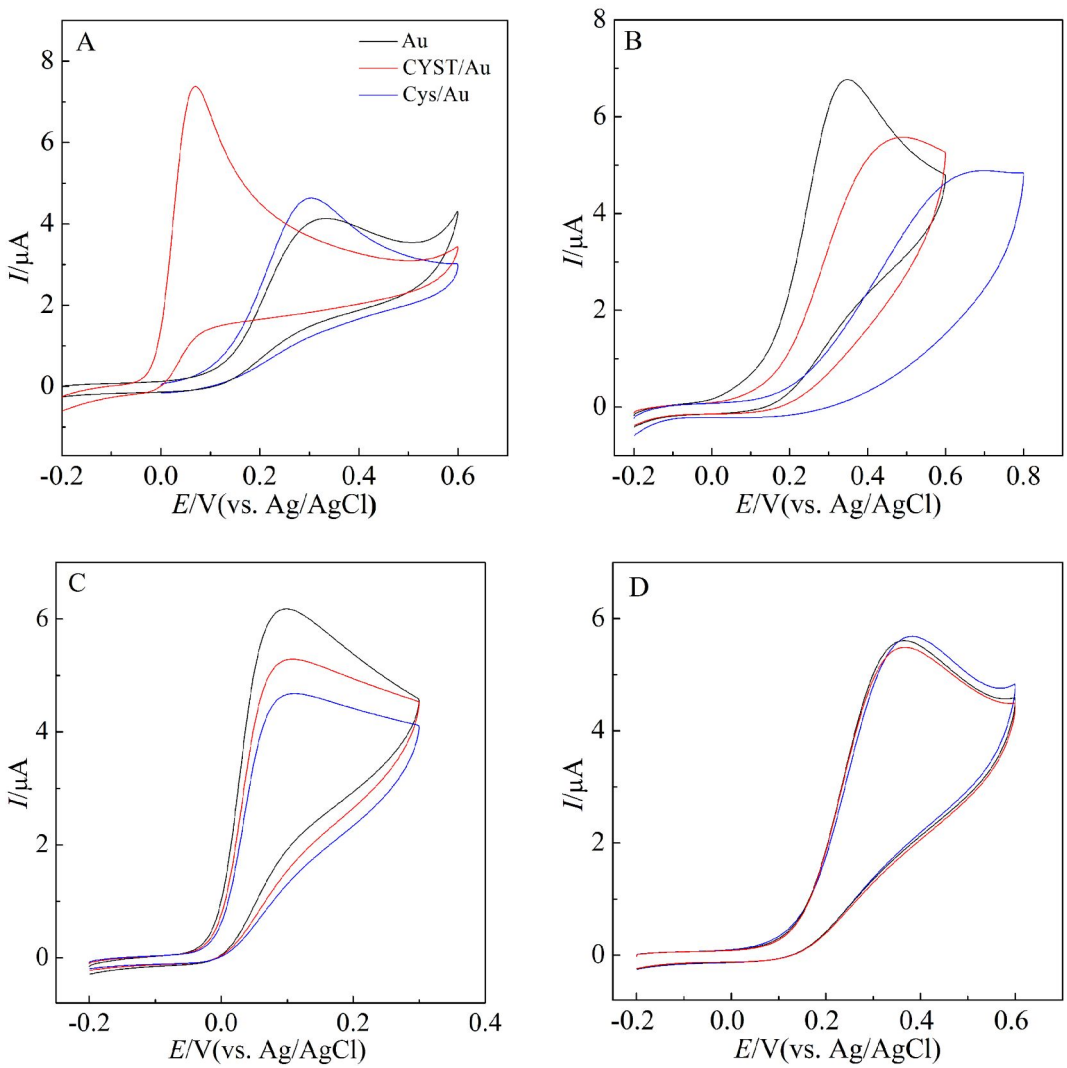

Fig. 1 (A) The CVs obtained at Au (black curve), Cys/Au (blue curve) and CYST/Au (red curve) in PBS solution containing 200 μmol·L^{-1} AA; CVs of (B) Au, (C) CYST/Au and (D) Cys/Au in PBS solutions containing 200 μmol·L^{-1} AA in the presence of 0 mg·mL^{-1} (black curve) BSA, 1 mg·mL^{-1} (red curve) BSA, and 2 mg·mL^{-1} (blue curve) BSA, scan rate 50 mV·s^{-1}.

(Cys-CYST/Au) was the optimal with the 73% remaining oxidation current (Figure 2B). From distribution of cysteine in three forms at different pH values in Figure 2C, we can see that the cysteine mainly existed in the form of zwitterions in pH 7.4 solution. The CYST monolayer is expected to be positively charged

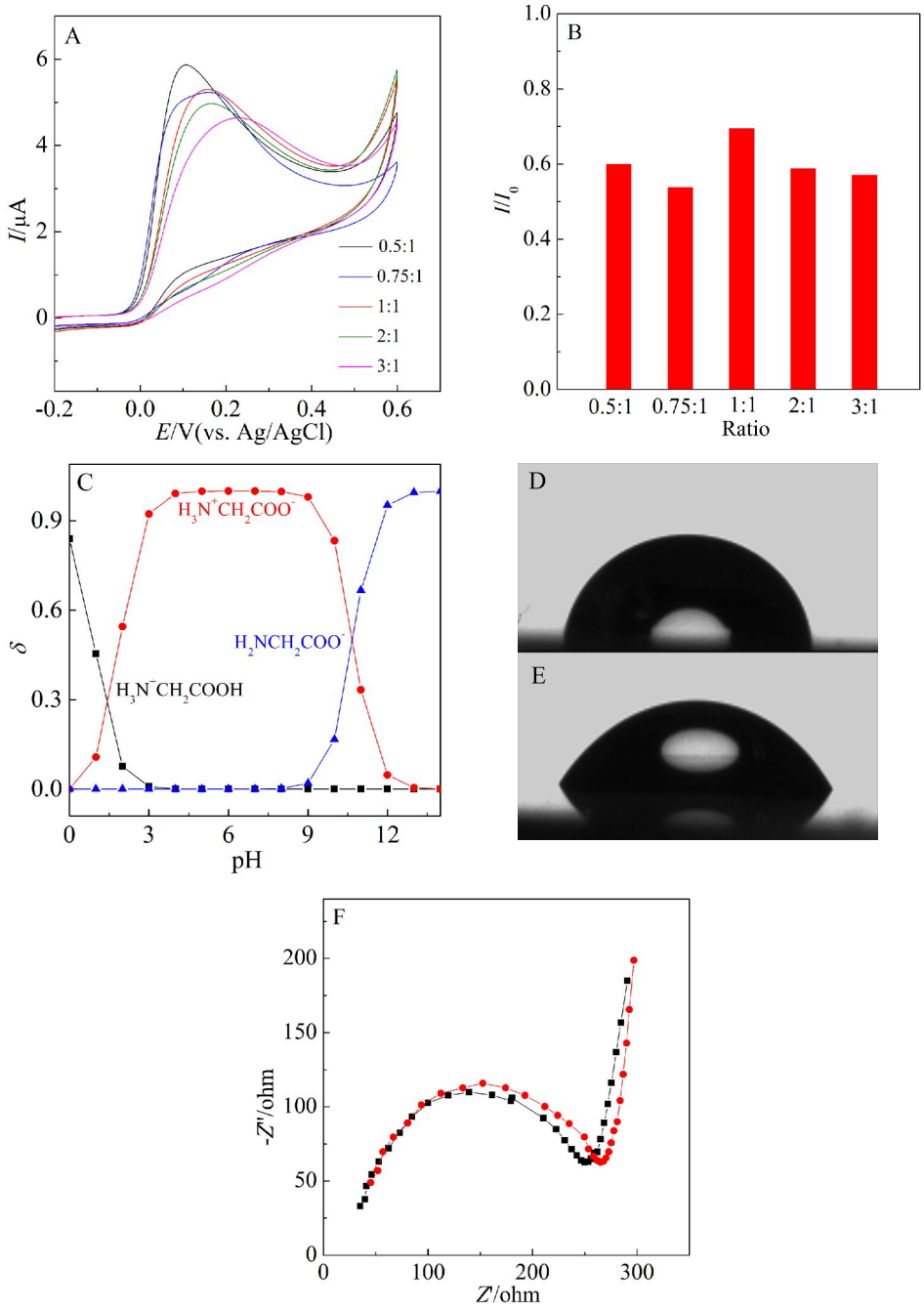

Fig. 2 (A) CVs obtained at Au electrodes modified with different ratios of cysteine and cystamine in PBS solution containing 200 μmol·L^{-1} AA. Scan rate, 50 mV·s^{-1}; (B) The remained amperometric oxidation current obtained at Au electrodes modified with different ratios of cysteine and cystamine in PBS solution (pH 7.4) containing 200 μmol·L^{-1} AA after adding 10 mg·mL^{-1} BSA. I_0 was the current response of 200 μmol·L^{-1} AA and I was the current response of 200 μmol·L^{-1} AA after addition of 10 mg·mL^{-1} BSA; (C) Relative proportion in different forms of cysteine (cation, anion and zwitterion) as a function of pH; Contact angles of (D) bare Au electrode and (E) Cys-CYST/Au; (F) The electrochemical impedance spectra of bare Au (black dotted curve) and Cys-CYST/Au (red dotted curve).

in phosphate buffer solution (pH 7.4) since the pKa of CYST is 8.35[31]. The contact angle experiments showed that the hydrophilicity of Cys-CYST/Au surface (contact angle, 57°) was obviously enhanced compared to bare Au (contact angle, 90°) (Figure 2D and Figure 2E), which might attribute to the good anti-protein adsorption performance of the co-self-assembled monolayer. From Figure 2F, the charge transfer resistance of Cys-CYST/Au (i.e., 219 ohm) is slightly larger than that of bare Au electrodes (i.e., 207 ohm), which indicates that Cys-CYST was assembled onto the surface of Au electrode because of nonconductive assembled membrane. Thus, the Cys-CYST/Au electrode exhibited fast electron transfer kinetics toward AA and good performance of anti-protein adsorption simultaneously.

We further applied the cysteine and cystamine co-self-assembled monolayers on gold microelectrodes (AuMEs) for *in vivo* detection. Figure 3A shows typical CVs of AuMEs with cysteine and cystamine co-self-assembled monolayers (Cys-CYST/AuMEs, the molar ratio, 1:1) in aCSF containing 200 μmol·L^{-1}

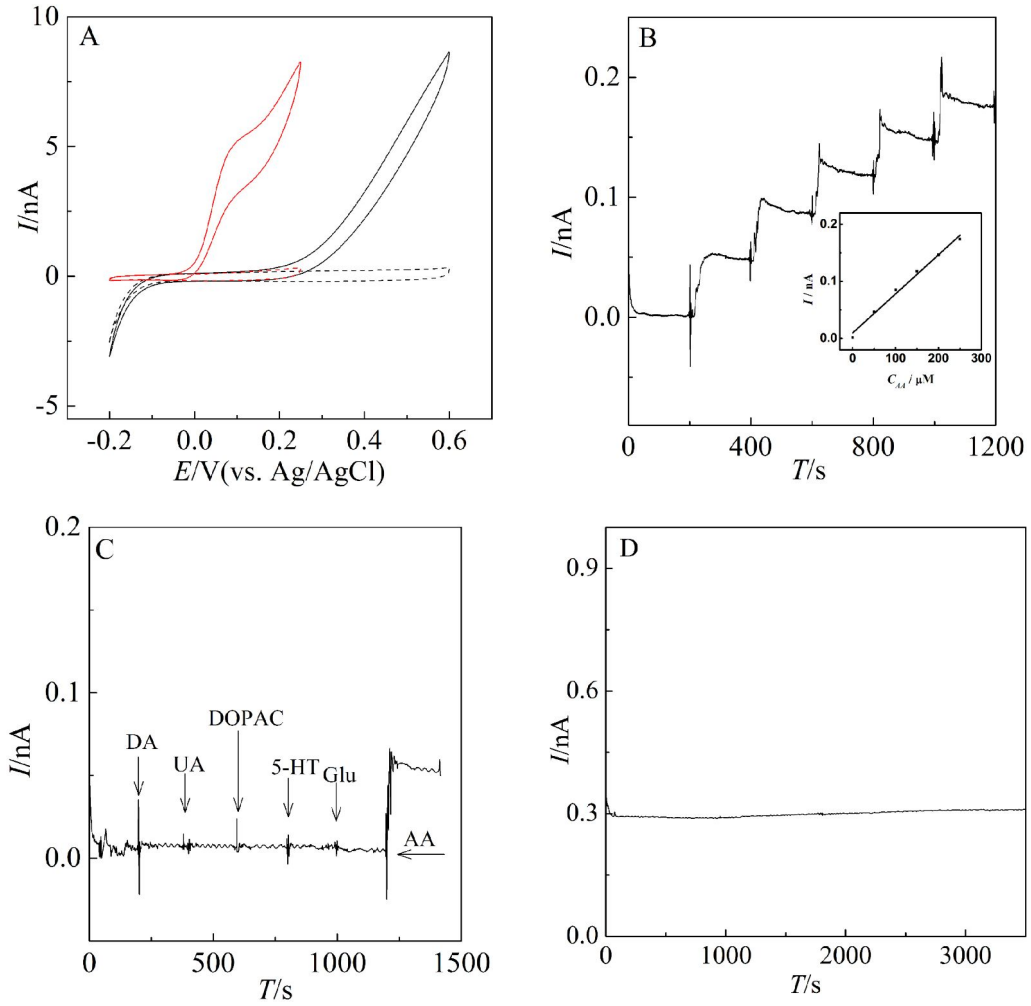

Fig. 3 (A) CVs obtained with AuMEs (black curve) and Cys-CYST/AuMEs (red curve) in aCSF in the absence (dotted curves) and the presence of 200 μmol·L^{-1} AA (solid curves). Scan rate, 50 mV·s^{-1}; (B) Amperometric current responses of the Cys-CYST/AuMEs toward successive addition of 50 μmol·L^{-1} AA in aCSF (pH 7.4). Insert, the calibration plot obtained from Fig. 3B; (C) Amperometric responses obtained at Cys-CYST/AuMEs in aCSF (pH 7.4) upon the additions of 10 μmol·L^{-1} DA, 20 μmol·L^{-1} UA, 20 μmol·L^{-1} DOPAC, 10 μmol·L^{-1} 5-HT, 50 μmol·L^{-1} Glu and 50 μmol·L^{-1} AA; (D) Amperometric response obtained at the Cys-CYST/AuMEs in aCSF containing 200 μmol·L^{-1} AA. Applied potential: 0.12 V·s^{-1} vs. Ag/AgCl.

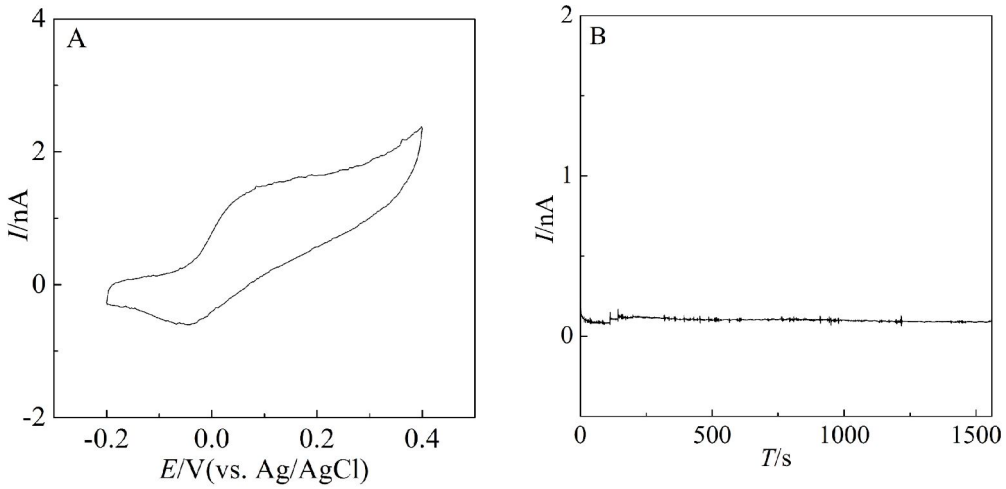

Fig. 4 (A) CV curve obtained at Cys-CYST/AuMEs in rat striatum. Scan rate, 50 mV·s^{-1}; (B) Amperometric response obtained at the Cys-CYST/AuMEs in rat striatum. Applied potential: 0.12 V·s^{-1} vs. Ag/AgCl.

AA. At bare AuMEs, the oxidation potential for AA was approximately 0.5 V vs. Ag/AgCl. In comparison, the CV response for 200 μmol·L^{-1} AA at the Cys-CYST/AuMEs showed a peak around 0.1 V. This might be due to the double layer effect on electrode reaction rate. When the monolayer is assembled on the electrode, the surface double layer structure is altered. The decreased thickness of double layer will increase the voltage drop and obtain faster kinetics and higher electrochemical sensitivity[32]. On the other hand, AA could be adsorbed on the surface of the electrode which will also induce peak current on microelectrode. In addition, the Cys-CYST/AuMEs produced the well-defined current responses in different concentrations of AA in Figure 3B. Current responded linearly with the concentration of AA within a range from 0 to 250 μmol·L^{-1} (I(nA) = 0.0096(nA) + 6.84×10^{-4} C_{AA}(μmol·L^{-1}), R^2 = 0.9879). Moreover, 10 μmol·L^{-1} DA, 20 μmol·L^{-1} UA, 20 μmol·L^{-1} DOPAC, 10 μmol·L^{-1} 5-HT, and 50 μmol·L^{-1} Glu, as a potential interferent in brain, were added into aCSF. The concentration of interferent is the maximum concentration in the brain, which is widely used in the reported literatures on *in vivo* analysis[20,23-24]. The Cys-CYST/AuMEs did not produce obvious current responses by other additives excluding AA as compared with those by 50 μmol·L^{-1} AA in Figure 3C, demonstrating the good selectivity for the AA. The stability of the Cys-CYST/AuMEs was also studied and the current response (0.32 nA) at Cys-CYST/AuMEs was quite stable for continuously sensing of 200 μmol·L^{-1} AA for almost 1 h (Figure 3D).

We further applied the co-self-monolayer to detect the basal concentration of AA in rat brain. The Cys-CYST/AuMEs showed a well-defined CV toward the oxidation of AA, and the peak potential was observed at about 0.10 V when the Cys-CYST/AuMEs was implanted in the rat striatum (Figure 4A). The similar peak potential of Cys-CYST/AuMEs toward AA *in vitro* in Figure 3A indicated that Cys-CYST/AuMEs remained the well self-assembled state after being implanted in the brain and had good selectivity for AA *in vivo*. Figure 4B shows typical current response *in vivo* on Cys-CYST/AuMEs, which was quite stable for about 0.5 h. Although the self-assembly membrane could be anti-fouling at some extent, the sensitivity would decrease *in vivo* electrochemistry. We used post-calibration method to accurately obtain the concentration of AA *in vivo*. According to the post-calibration curve, the basal concentration of AA in rat striatum was determined to be 257 ±30 μmol·L^{-1} (n = 3), which was consistent with the reported values using other methods[20-21,31]. These results demonstrated that the strategy of cysteine and cystamine co-self-monolayer on AuMEs is a simple and effective method for *in vivo* detection of AA.

3 Conclusions and Future Perspectives

We developed a simple and effective method of cysteine and cystamine co-self-assembled monolayer on AuMEs to *in vivo* detect AA. As a result, we found that the ratio of cysteine and cystamine at 1:1 was the optimal molar ratio in co-self-assembled monolayer for detection of AA at low potential and that the co-self-assembled monolayer showed anti-adsorption of nonspecific proteins at some extent. The co-self-assembled monolayer on the AuMEs exhibited excellent selectivity and stability for measurement of AA, and the basal concentration of AA was obtained in rat striatum successfully. Our method has provided a potential strategy for detections of other neurotransmitters and neuromodulators in CNS. Moreover, our strategy has many potential applications. For example, it can be used as a blocking agent and a protective agent for electrochemical immunosensor, which can improve the sensitivity of the sensor, or it can be modified on the surface of gold nanoparticles to improve anti-fouling performance.

Acknowledgements

We gratefully acknowledge the financial supports from the National Natural Science Foundation of China (Grant No. 21874152) and Renmin University of China.

References:

[1] Ulman A. Wetting studies of molecularly engineered surfaces[J]. Thin Solid Films, 1996, 273(1/2): 48-53.

[2] Cook K M, Nissley D A, Ferguson G S. Spatially selective formation of hydrocarbon, fluorocarbon, and hydroxyl-terminated monolayers on a microelectrode array[J]. Langmuir, 2013, 29(23): 6779-6783.

[3] Chaki N K, Vijayamohanan K. Self-assembled monolayers as a tunable platform for biosensor applications[J]. Biosensors and Bioelectronics, 2002, 17(1/2): 1-12.

[4] Tencer M, Olivieri A, Tezel B, et al. Chip-scale electrochemical differentiation of SAM-coated gold features using a probe array[J]. Journal of The Electrochemical Society, 2012, 159(3): J77-J82.

[5] Whitesides G M, Ostuni E, Takayama S, et al. Soft lithography in biology and biochemistry[J]. Annual Review of Biomedical Engineering, 2001, 3(1): 335-373.

[6] Gonçalves I C, Martins M C L, Barbosa M A, et al. Protein adsorption on 18-alkyl chains immobilized on hydroxyl-terminated self-assembled monolayers[J]. Biomaterials, 2005, 26(18): 3891-3899.

[7] Besharat Z, Wakeham D, Johnson C M, et al. Mixed monolayers of alkane thiols with polar terminal group on gold: Investigation of structure dependent surface properties[J]. Journal of Colloid and Interface Science, 2016, 484: 279-290.

[8] Yang W, Gooding J J, Hibbert D B. Characterisation of gold electrodes modified with self-assembled monolayers of L-cysteine for the adsorptive stripping analysis of copper[J]. Journal of Electroanalytical Chemistry, 2001, 516 (1/2): 10-16.

[9] Zhang H M, Li N Q. The direct electrochemistry of myoglobin at a DL-homocysteine self-assembled gold electrode[J]. Bioelectrochemistry, 2001, 53(1): 97-101.

[10] Meng X Y, Wu X Q, Wang Z S, et al. The electrochemical and spectroelectrochemical behaviors of SOD at cysteine modified gold electrode[J]. Bioelectrochemistry, 2001, 54 (2): 125-129.

[11] Hoshi T, Anzai J, Osa T. Electrochemical deposition of avidin on the surface of a platinum electrode for enzyme sensor applications[J]. Analytica Chimica Acta, 1994, 289 (3): 321-327.

[12] Fägerstam L G, Frostell-Karlsson A, Karlsson R, et al. Biospecific interaction analysis using surface plasmon resonance detection applied to kinetic, binding site and concentration analysis[J]. Journal of Chromatography A, 1992, 597(1/2): 397-410.

[13] Sugawara T, Matsuda T. Development of a novel protein fixation method with micron-order precision[J]. Langmuir, 1995, 11(6): 2267-2271.

[14] Xiao T F, Wu F, Hao J, et al. *In vivo* analysis with electrochemical sensors and biosensors[J]. Analytical Chemistry, 2016, 89(1): 300-313.

[15] Ding C Q, Zhu A W, Tian Y. Functional surface engineering of C-dots for fluorescent biosensing and *in vivo* bioimaging[J]. Accounts of Chemical Research, 2013, 47 (1): 20-30.

[16] Zhou L, Ding H, Yan F, et al. Electrochemical detection of Alzheimer's disease related substances in biofluids by silica nanochannel membrane modified glassy carbon electrodes[J]. Analyst, 2018, 143(19): 4756-4763.

[17] Guan L H(关利浩), Wang C(王超), Zhang W(张望), et al. A facile strategy for two-step fabrication of gold nanoelectrode for *in vivo* dopamine detection[J]. Journal of

Electrochemistry(电化学), 2019, 25(2): 244-251.
[18] Saleh F S, Okajima T, Mao L Q(毛兰群), et al. Development of dehydrogenase-based bioanode using poly (phenosafranin)-functionalized SWCNT nanocomposites and its application to ethanol biosensor[J]. Journal of Electrochemistry(电化学), 2011, 17(3): 263-270.
[19] Zhang Z P, Lin Y Q, Mao L Q. On-line electrochemical measurements of cerebral hypoxanthine of freely moving rats[J]. Science in China Series B: Chemistry, 2009, 52(10): 1677-1682.
[20] Zhang M N, Liu K, Gong K P, et al. Continuous on-line monitoring of extracellular ascorbate depletion in the rat striatum induced by global ischemia with carbon nanotube-modified glassy carbon electrode integrated into a thin-layer radial flow cell[J]. Analytical Chemistry, 2005, 77(19): 6234-6242.
[21] Cheng H J, Li L J, Zhang M N, et al. Recent advances on *in vivo* analysis of ascorbic acid in brain functions[J]. TrAC Trends in Analytical Chemistry, 2018, 109: 247-259.
[22] Wu F, Cheng H J, Wei H, et al. Galvanic redox potentiometry for self-driven *in vivo* measurement of neurochemical dynamics at open-circuit potential[J]. Analytical Chemistry, 2018, 90(21): 13021-13029.
[23] Liu X M, Zhang M N, Xiao T F, et al. Protein pretreatment of microelectrodes enables *in vivo* electrochemical measurements with easy precalibration and interference-free from proteins[J]. Analytical Chemistry, 2016, 88 (14): 7238-7244.
[24] Liu X M, Xiao T F, Wu F, et al. Ultrathin cell-membrane-mimic phosphorylcholine polymer film coating enables large improvements for *in vivo* electrochemical detection [J]. Angewandte Chemie International Edition, 2017, 56 (39): 11802-11806.
[25] Ostuni E, Chapman R G, Holmlin R E, et al. A survey of structure—property relationships of surfaces that resist the adsorption of protein[J]. Langmuir, 2001, 17(18): 5605-5620.
[26] Lin P, Ding L, Lin C W, et al. Nonfouling property of zwitterionic cysteine surface[J]. Langmuir, 2014, 30(22): 6497-6507.
[27] Ostuni E, Chapman R G, Holmlin R E, et al. A survey of structure-property relationships of surfaces that resist the adsorption of protein[J]. Langmuir, 2001, 17(18): 5605-5620.
[28] Xiang L, Yu P, Zhang M N, et al. Platinized aligned carbon nanotube-sheathed carbon fiber microelectrodes for *in vivo* amperometric monitoring of oxygen[J]. Analytical Chemistry, 2014, 86(10): 5017-5023.
[29] Zhang M N, Liu K, Xiang L, et al. Carbon nanotube-modified carbon fiber microelectrodes for *in vivo* voltammetric measurement of ascorbic acid in rat brain [J]. Analytical chemistry, 2007, 79(17): 6559-6565.
[30] Raj C R, Tokuda K, Ohsaka T. Electroanalytical applications of cationic self-assembled monolayers: square-wave voltammetric determination of dopamine and ascorbate [J]. Bioelectrochemistry, 2001, 53(2): 183-191.
[31] Molinero V, Calvo E J. Electrostatic interactions at self assembled molecular films of charged thiols on gold[J]. Journal of Electroanalytical Chemistry, 1998, 445(1/2): 17-25.
[32] Cheng C A, Brajter-Toth A. Permselectivity and high sensitivity at ultrathin monolayers. Effect of film hydrophobicity[J]. Analytical Chemistry, 1995, 67(17): 2767-2775.

L-半胱氨酸和胱胺共自组装膜活体检测抗坏血酸

张 悦,冯涛涛,纪文亮,张美宁*
(中国人民大学化学系,北京 100872)

摘要: 自组装单分子膜(SAM)由于其独特的物理化学性质近年来受到了极大的关注. SAM 通过金硫键在电极表面形成高度有序的单分子膜,该稳定的分子膜不仅可以调节表面的亲疏水性质,而且可以促进电极表面氧化还原活性分子的反应速率. 本论文提出了一种简单有效的方法,在金微电极上构建半胱氨酸和胱胺共自组装单分子膜用于活体内抗坏血酸的检测. 研究发现,当混合单分子层中半胱氨酸和胱胺的摩尔比为 1:1 时,可以在低电位下(约为 0.10 V)显著增强抗坏血酸氧化的电子转移动力学,同时该膜能在一定程度上抵抗蛋白质在电极表面的非特异性吸附. 将共自组装单分子膜应用到活体检测中, 作者检测到鼠纹状体中抗坏血酸的基准值为 257±30 μmol·L^{-1}(n = 3). 本论文为活体电化学检测提供了一种简单、有效的方法.

关键词: L-半胱氨酸和胱胺;共自组装膜;抗坏血酸;抗吸附;活体